



Acetate Acetylacetonate Ampy Ruthenium(II) Complexes as Efficient Catalysts for Ketone Transfer Hydrogenation

Daniela A. Hey,^[a] Michael J. Sauer,^[a] Pauline J. Fischer,^[a] Eva-Maria H. J. Esslinger,^[a] Fritz E. Kühn,^{*[a]} and Walter Baratta^{*[b]}

The mixed acetate acetylacetonate (acac) ruthenium(II) phosphine complexes $\text{Ru}(\text{OAc})(\text{acac})\text{P}_2$ [$\text{P}_2 = (\text{PPh}_3)_2$, $\text{Ph}_2\text{P}(\text{CH}_2)_4\text{PPh}_2$ (dppb)] were prepared by protonation of $\text{Ru}(\text{OAc})_2(\text{PPh}_3)_2$ with acetylacetonate in dichloromethane. Reaction of the dppb derivative with 2-(aminomethyl)pyridine (ampy) affords the complex $\text{Ru}(\text{OAc})(\text{acac})(\text{ampy})(\text{dppb})$, which converts to $[\text{Ru}(\text{acac})(\text{ampy})(\text{dppb})](\text{OAc})$ in toluene at 90°C . In the former derivative the ampy ligand is monodentate and coordinates

through the NH_2 -moiety. The isolated acac complexes are active catalysts for the transfer hydrogenation of ketones with loadings as low as 0.01 mol%, the ampy having a strong accelerating effect. Several aromatic and aliphatic ketone substrates are converted to their corresponding alcohols, and different electronic influences through substituents on acetophenone are tolerated.

Introduction

Ruthenium diphosphine complexes bearing carboxylate ligands have widely been explored during the last decades with particular attention to their activity in the catalytic hydrogenation (HY).^[1] The well-known acetate complexes $\text{Ru}(\text{OAc})_2\text{P}_2$ ^[2] are usually prepared from the commercially available precursors $\text{RuCl}_2(\text{PPh}_3)_3$, $[\text{RuCl}_2(\text{cod})]_n$ (cod = 1,5-cyclooctadiene) or $[\text{RuCl}_2(p\text{-cymene})]_2$, by exchange of chloride with carboxylate and reaction with phosphines. The resulting complexes have found application as catalysts for hydrogenation of olefins and functionalized ketones, with Noyori's $\text{Ru}(\text{OAc})_2[(S)\text{-BINAP}]$ being one of the most popular systems used in asymmetric HY.^[3] In addition, carboxylate ruthenium(II) catalysts bearing strong coordinating carbene and pincer ligands have been reported to display high productivity in HY and transfer hydrogenation (TH) of carbonyl compounds.^[4] Conversely, the related acetylacetonate phosphine ruthenium(II) complexes are generally synthe-

sized from $\text{Ru}(\text{acac})_3$ ^[5] (acac = acetylacetonate) and phosphines in presence of reducing agents (i.e. zinc or PR_3).^[6] The *in situ* preparation of $\text{Ru}(\text{acac})_2\text{P}_2$ systems for HY reactions has been reported for $\text{P}_2 = \text{dppm}$, dppe, dppp, dppf and BINAP (Figure 1).^[6–7]

Complexes containing chiral diphosphines have been described to catalyze the asymmetric HY of alkenes and amides at relatively high catalyst loading, under high hydrogen pressure and with moderate turnover frequencies (TOFs).^[7–8] Comparison of the performance of the acetate $\text{Ru}(\text{OAc})_2\text{P}_2$ vs. the corresponding acetylacetonate $\text{Ru}(\text{acac})_2\text{P}_2$ complexes shows that acac derivatives are significantly less active. Interestingly, the catalytic activity of $\text{Ru}(\text{acac})_2[(S)\text{-BINAP}]$ in olefin HY can be considerably increased by reaction with carboxylic acid under visible light for several days, leading to the mixed carboxylate and acetylacetonate species $\text{Ru}(\text{OCOR})(\text{acac})[(S)\text{-BINAP}]$, which is also more active than the diacetate catalyst $\text{Ru}(\text{OAc})_2[(S)\text{-BINAP}]$ (Scheme 1).^[8b,9]

Considering the high reactivity of ruthenium(II) acetate phosphine complexes and the contrasting robustness of their acetylacetonate analogues in catalysis, the heteroleptic acetate/acetylacetonate ruthenium(II) complexes were assumed to offer reactivity as well as stability, both beneficial for catalysis. Lability of an anionic ligand is crucial to open a free coordination site for the substrate, while the stability of the catalyst's backbone is important to reach high turnover numbers (TONs). In this way a very efficient and at the same time highly robust catalyst can

[a] D. A. Hey, M. J. Sauer, P. J. Fischer, E.-M. H. J. Esslinger, Prof. F. E. Kühn
Molecular Catalysis, Catalysis Research Center and Department of Catalysis
Technische Universität München
Lichtenbergstr. 4
85748 Garching, München (Germany)
E-mail: fritz.kuehn@ch.tum.de

[b] Prof. W. Baratta
Dipartimento di Scienze AgroAlimentari, Ambientali e Animali (DIA A)
Università di Udine
Via Cotonificio 108
33100 Udine (Italy)
E-mail: walter.baratta@uniud.it

Supporting information for this article is available on the WWW under
<https://doi.org/10.1002/cctc.202000542>

This publication is part of a joint Special Collection with EurJIC on "Pincer Chemistry & Catalysis". Please follow the link for more articles in the collection.

© 2020 The Authors. Published by Wiley-VCH Verlag GmbH & Co. KGaA. This is an open access article under the terms of the Creative Commons Attribution Non-Commercial NoDerivs License, which permits use and distribution in any medium, provided the original work is properly cited, the use is non-commercial and no modifications or adaptations are made.

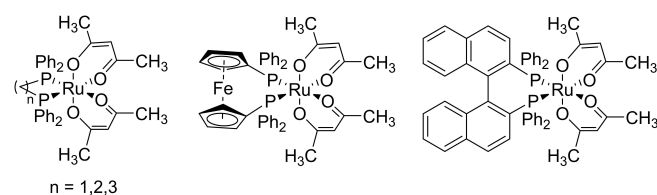
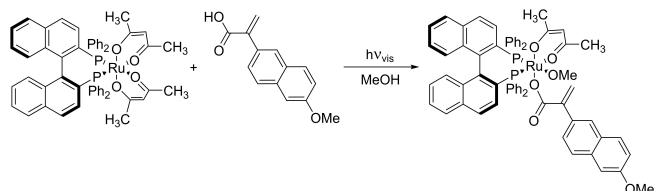


Figure 1. Acetylacetonate diphosphine ruthenium(II) complexes.



Scheme 1. Light activation of Ru(acac)₂[(S)-BINAP] for the HY of alkenes.

be achieved without requiring the time-consuming activation process that had to be performed previously.^[8b] Notably, mixed acetate/acetylacetonate phosphine complexes of ruthenium(II) are sparingly reported in literature.^[8b]

It is well known that addition of amines to ruthenium(II) phosphine complexes leads to an increase of the performance in HY and transfer hydrogenation (TH) of carbonyl compounds.^[4b,10] In particular, while ethylenediamine (en) has been employed to increase the activity in the HY of ketones, 2-(aminomethyl)pyridine (ampy)^[2c,11] affords extremely active catalysts in the TH. In these cases the presence of an NH function plays a pivotal role, leading to a rapid reduction via outer sphere mechanism.^[12] In addition, ampy based ruthenium(II) complexes are well-established as active catalysts for a number of organic transformations (dehydrogenation, racemization, deuteration, isomerization).^[13]

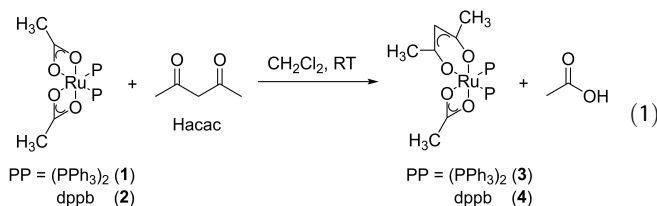
In order to obtain highly active and productive catalysts with retarded deactivation, the design of complexes combining both labile and robust ligands is crucial. In addition, a straightforward preparation of the catalysts, avoiding multiple steps, tedious and costly ligand preparation,^[14] appears to be fundamental for applications.

In this work a simple synthetic route for the preparation of mixed acetate/acetylacetonate ruthenium phosphine complexes Ru(OAc)(acac)P₂ and their reaction with the ampy ligand is reported. The isolated and *in situ* formed ampy derivatives display high activity in the TH of ketones.

Results and Discussion

Syntheses

Reaction of the diacetate ruthenium(II) triphenylphosphine complex Ru(OAc)₂(PPh₃)₂ (**1**) with acetylacetonate (Hacac, 1.5 equiv.) in dichloromethane at room temperature for 3 h affords the mixed acetate/acetylacetonate complex **3** in 68% yield (Eq. 1).



In CDCl₃, **3** causes two doublets in the ³¹P{¹H} spectrum at δ = 64.9 and 53.5 ppm (²J(PP) = 36.4 Hz), in accordance with the two chemically non-equivalent phosphine moieties in *trans* position to the acetate and acac ligand. The moiety in *trans* position to the acetate is low-field shifted in comparison to the one *trans* to acac, as inferred by comparison of the chemical shifts of analogue di-acetate and -acac complexes (vide infra and refs.^[1d,15]). The ¹H NMR spectrum shows three distinct CH₃ signals for the two acac and the acetate methyl groups at δ = 1.69, 1.59 and 1.47 ppm.

Reaction of the related diacetate ruthenium(II) diphosphine complex Ru(OAc)₂(dppb) (**2**) with acetylacetonate in dichloromethane at room temperature for 3 h affords complex **4** in 63% yield (Eq. 1). In the ³¹P{¹H} spectrum, **4** exhibits two doublets at δ = 66.8 and 52.6 ppm (²J(PP) = 43.2 Hz), in accordance with the two chemically non-equivalent phosphine moieties in *trans* position to the acetate and acac ligand, respectively. The ¹H NMR spectrum shows three distinct signals for the CH₃ groups of the two acac and the acetate methyl groups at δ = 1.68, 1.52 and 1.45 ppm.

The structure of complex **4** is further confirmed by SC-XRD measurements (Figure 2). Accordingly, the ruthenium(II) center is coordinated pseudo-octahedrally by the chelating dppb, acetate and acac ligands.

As expected, the Ru–O bond lengths in *trans* position to the phosphine moieties are slightly longer (Ru1–O1 = 2.232(3) Å, Ru1–O4 = 2.110(3) Å) compared to those *trans* to another oxygen atom (Ru1–O2 = 2.128(3) Å, Ru1–O3 = 2.062(3) Å) due to the strong *trans* influence of the phosphine. The shorter Ru–O bond lengths of acac vs. OAc and their smaller variations (Ru1–O4–Ru1–O3 = 0.048 Å vs. Ru1–O1–Ru1–O2 = 0.104 Å) indicate that acac is coordinated stronger with respect to OAc, which is more susceptible to the electronic properties of the *trans* ligand. Electron delocalization of the acac ligand is manifested by bond lengths for the carbon backbone that lie in the range of aromatic C–C bonds (C3–C4 = 1.393(7) Å, C4–C5 = 1.403(7) Å).

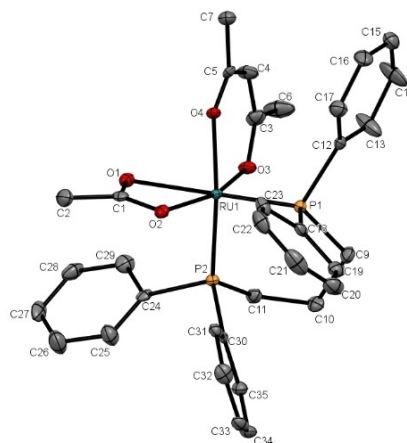
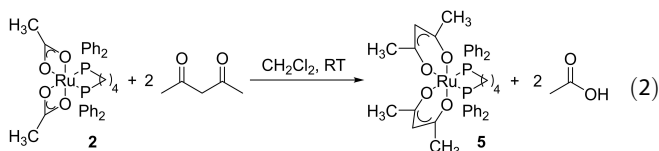


Figure 2. ORTEP-style drawing of **4** with ellipsoids at 50% probability level. Hydrogen atoms omitted for clarity. For selected bond lengths and angles see Supporting Information.

The di-acac complex **5** was synthesized by adding an excess of Hacac (6 equiv.) to **2** at room temperature in dichloromethane for 3 d and isolated in 58% yield (Eq. 2). The formation of **5** instead of **4** occurs due to the high excess of Hacac, as well as to the prolonged reaction time, which results in the gradual substitution of both OAc ligands from **2**.



In solution, **5** exhibits a sharp singlet at $\delta=52.9$ ppm in the $^{31}\text{P}\{^1\text{H}\}$ NMR spectrum for the symmetrically substituted dppb ligand. The ^1H and ^{13}C spectra further confirm the formation of a single product with two distinct CH_3 moieties at $\delta=1.65$ and 1.46 ppm in the proton spectrum and a CH signal at $\delta=98.8$ ppm for the tertiary carbon atom of the enol form of the acac ligands.

The SC-XRD structure of **5** (Figure 3) shows the ruthenium (II) center in a pseudo-octahedral coordination geometry, with the chelating dppb and two acac ligands. Similar to complex **4**, the acac ligand coordinates strongly to the ruthenium center, indicated by the relatively short Ru–O bonds.

Treatment of **4** with an excess of ampy (6 equiv.) in dichloromethane at room temperature affords complex **6** in 77% isolated yield via an equilibrium reaction (Scheme 2).

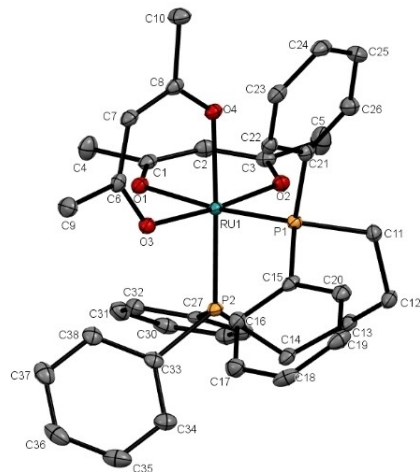
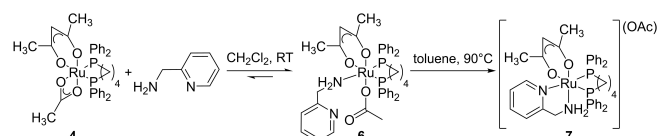


Figure 3. ORTEP-style drawing of **5** with ellipsoids at 50% probability level. Hydrogen atoms omitted for clarity. For selected bond lengths and angles see Supporting Information.



Scheme 2. Synthesis of **6** and **7** from **4** with ampy.

In toluene- d_8 , **6** exhibits two doublets at $\delta=53.2$ and 45.9 ppm ($^2J(\text{PP})=38.2$ Hz) in the $^{31}\text{P}\{^1\text{H}\}$ NMR spectrum for the phosphine moieties in *trans* position to the acac and amine ligand, respectively. In the ^1H NMR spectrum, two singlets at $\delta=1.64$ and 1.33 ppm evidence the CH_3 moieties of the acac ligand. The acetate- CH_3 appears downfield-shifted at $\delta=2.16$ ppm, while the NH_2 protons lead to signals at $\delta=3.98$ and $6.92\text{--}6.97$ ppm, the latter being involved in hydrogen bonding to the acetate. The multiplets at $\delta=3.77$ and 3.37 ppm are in accord with the diastereotopic CH_2NH_2 protons.

The SC-XRD structure of **6** (Figure 4) shows the ruthenium (II) center in a pseudo-octahedral coordination geometry, with bidentate phosphine and acac ligands and monodentate coordination modes of the acetate and ampy moieties.

The Ru–O bonds to acac in **6** are slightly longer than in complex **4** (vide supra), while the Ru–O bond length to acetate decreases moderately for **6** (Ru1–O1=2.1061 Å). Two of the phenyl rings of dppb exhibit a planar arrangement to each other (C24–C29 and C36–C41), indicating π -stacking between the aromatic rings. An intramolecular hydrogen bond between the acetate C=O and the ampy NH stabilizes complex **6** via a six-membered ring (O2–H1N distance=2.172 Å).^[16] At room temperature, **6** dissociates in CD_2Cl_2 to **4** and ampy through an equilibrium reaction (Scheme 2) with a **6**:**4** molar ratio of about 5, whereas in toluene- d_8 the **6**:**4** ratio is 10, as inferred by $^{31}\text{P}\{^1\text{H}\}$ NMR measurements (see Supporting Information). At temperatures lower than -10°C in toluene- d_8 , **6** does practically not dissociate, while upon heating above 50°C , the new species **7** forms (Scheme 2 and Supporting Information). The cationic complex **7** was isolated in 85% yield by heating **6** at 90°C in toluene for 1 h. The $^{31}\text{P}\{^1\text{H}\}$ NMR spectrum of **7** in toluene- d_8 shows two doublets at $\delta=51.0$ and 45.6 ppm ($^2J(\text{PP})=36.8$ Hz) for the phosphine moieties in *trans* position to the acac and pyridine ligand, respectively. In the ^1H NMR spectrum,

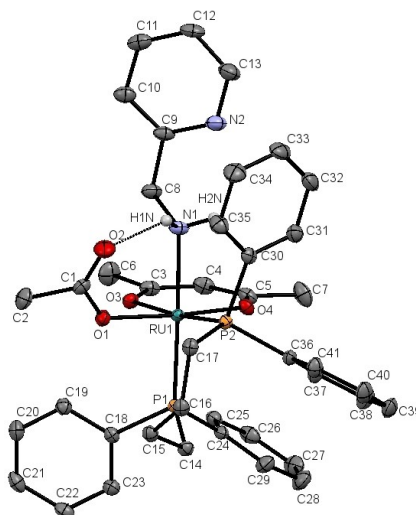


Figure 4. ORTEP-style drawing of **6** with ellipsoids at 50% probability level. All hydrogen atoms except H1N and H2N, and co-crystallized CH_2Cl_2 are omitted for clarity. Hydrogen atoms were calculated in ideal positions (riding model). For selected bond lengths and angles see Supporting Information.

two singlets at $\delta = 1.94$ and 1.02 ppm are in accordance with the acac-CH₃ moieties. The CH₃ group of the acetate anion occurs downfield shifted at $\delta = 2.53$ ppm. The diastereotopic CH₂NH₂ protons of the ampy ligand appear at $\delta = 3.74$ ppm (m) and 3.53 ppm (dd, $^2J = 18.18$ Hz, $^3J = 8.34$ Hz), while the multiplets at $\delta = 3.33$ and 8.56 ppm evidence the amine protons, the latter signal being ascribed to hydrogen bonding of one amine proton to an oxygen atom of the acetate. Bidentate coordination of ampy in **7** results in a high-field shift of the pyridine proton signals in comparison to its monodentate analogue **6** ($\Delta\delta_{\text{max}} = 0.87$ ppm). The SC-XRD structure of **7** shows that the ruthenium(II) center is pseudo-octahedrally coordinated by bidentate dppb, acac and ampy ligands with acetate as counterion (Figure 5). By difference to **6**, the NH₂ moiety of **7** is coordinated *trans* to oxygen, indicating that **7** forms from **6** through reorganization of the ampy ligand. The short NH–O distance (H2N–O1 = 2.039 Å) indicates a strong hydrogen bond between the outer sphere acetate and the cationic complex, in accordance with the NMR data in solution.

Thus, the syntheses of ruthenium(II) diphosphine complexes with diacetylacetonate and mixed acetate/acetylacetonate anionic ligands were accomplished by protonation of the diacetate phosphine precursors. Addition of ampy to the mixed complex leads to mono- or bidentate binding of ampy through opening or de-coordination of acetate.

Catalytic transfer hydrogenation

The catalytic activities of the diacetate, diacetylacetonate and mixed acetate/acetylacetonate complexes **1–7** were investigated in the TH of acetophenone (**a**) in ⁱPrOH with NaOⁱPr as base (Scheme 3).

At 0.1 mol% catalyst loading, the diacetate complexes **1** and **2** exhibit moderate catalytic performance, reaching 38 and 53% conversion of **a** in 8 h, respectively (Table 1, entries 1 and 2). Complex **2** with the bidentate phosphine is more active than

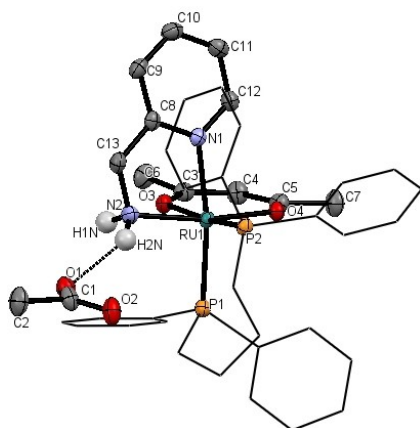
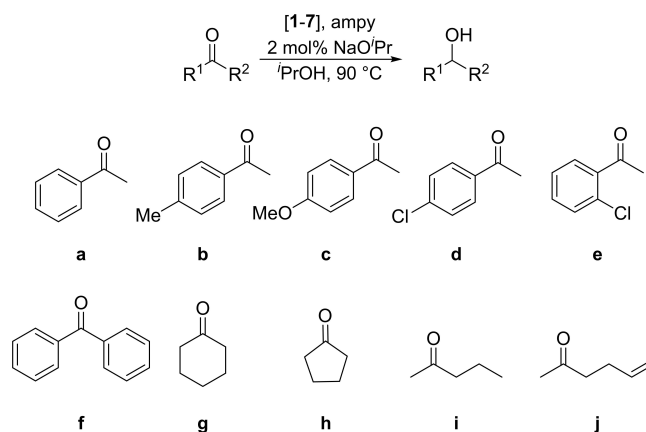


Figure 5. ORTEP-style drawing of **7** with ellipsoids at 50% probability level. All hydrogen atoms except H1N and H2N are omitted for clarity. Hydrogen atoms were calculated in ideal positions (riding model). For selected bond lengths and angles see Supporting Information.



Scheme 3. Transfer hydrogenation of ketones **a–j** catalyzed by **1–7** in ⁱPrOH at 90 °C oil bath temperature with NaOⁱPr.

Table 1. Transfer hydrogenation of **a** with complexes **1–5**.^[a]

| Entry | Catalyst | Additive ^[b] | Conversion ^[c] [%] | Time [min] | TOF ^[d] [h ⁻¹] |
|-------|----------|-------------------------|-------------------------------|------------|---------------------------------------|
| 1 | 1 | – | 38 | 480 | n.d. |
| 2 | 2 | – | 53 | 480 | 100 |
| 3 | 3 | – | 28 | 480 | n.d. |
| 4 | 4 | – | 75 | 480 | 930 |
| 5 | 5 | – | 1 | 480 | n.d. |
| 6 | 1 | ampy | 91 | 60 | 3,300 |
| 7 | 2 | ampy | 97 | 60 | 2,200 |
| 8 | 3 | ampy | 93 | 60 | 15,000 |
| 9 | 4 | ampy | 98 | 5 | 26,000 |
| 10 | 5 | ampy | 4 | 480 | n.d. |

[a] Conditions: ⁱPrOH, 1 mmol **a**, 2 mol% NaOⁱPr, 0.1 mol% catalyst, S/C/B = 100/0.1/2, [b] 10 equiv. additive with respect to the catalyst, [c] Maximum conversion, determined by GC; conversion corresponds to yield of 1-phenylethanol, [d] Calculated at 50% conversion.

the triphenylphosphine complex **1**, although none of these catalyst derivatives leads to full conversion of **a**. The comparison of the activity of the mixed acetate/acac complexes **3** and **4** with PPh₃ and dppb ancillary ligands (Table 1, entries 3 and 4) highlights the beneficial effect of the chelating dppb with respect to the monodentate PPh₃. Thus, **3** converts a maximum of 28% **a**, while **4** reaches 75% conversion in 8 h. The low conversion with **3** is attributed to catalyst deactivation upon dissociation of the phosphine, inhibited in **4** by the bidentate phosphine. The di-acac complex **5** is virtually inactive, converting only 1% **a** within 8 h (Table 1, entry 5). This is likely due to the strong bonding of acac to ruthenium, preventing the generation of a free coordination site and formation of the active catalytic species.

Upon addition of 10 equiv. ampy to the reaction mixture, **1–4** reach quantitative conversion within 60 min (**1–3**, Table 1, entries 6–8) and 5 min (**4**, Table 1, entry 9), with turnover frequencies (TOFs) of 3,300 h⁻¹ (**1**), 2,200 h⁻¹ (**2**), 15,000 h⁻¹ (**3**) and 26,000 h⁻¹ (**4**). The fastest conversion is obtained with the mixed acetate/acac complex **4**, while both, the diacetate complexes **1** and **2**, and the PPh₃ analogue **3**, fall short in comparison. The di-acac complex **5** still shows no considerable conversion upon addition of ampy (4% conversion within 8 h,

entry 10). Control $^{31}\text{P}\{^1\text{H}\}$ NMR measurements show no reaction of **5** with ampy at 90°C in $i\text{PrOH}$. In absence of ruthenium catalysts, the base NaO^iPr (2 mol%) is not capable of converting the substrate (1% conversion within 8 h). Without base, the most active catalyst **4** shows no activity, while ampy (1 mol%) is further inactive, reaching 3% conversion within 8 h. These results indicate that basic conditions are crucial for the formation of the active species.

Primary amines, like benzylamine (bza) or ethylenediamine (en), also exhibit considerable impact on catalyst **4** (Figure 6). Bza (\blacktriangle green) (10 equiv.) slows down the reaction ($\text{TOF} = 700\text{ h}^{-1}$), and low conversion is observed (57% conversion in 60 min). Addition of en (\blacksquare orange) considerably pushes the catalyst's performance ($\text{TOF} = 2,900\text{ h}^{-1}$), although the performance is lower with respect to the one obtained with ampy (x blue) ($\text{TOF} = 26,000\text{ h}^{-1}$).

At lower loading of **4** (0.03 mol%) in presence of ampy (2–10 equiv.) **a** is quantitatively converted to 1-phenylethanol (Table 2, entries 1 and 2). To investigate the impact of ampy, different equivalents of this additive with respect to the catalyst were applied. With 2 and 10 equiv. ampy, 96% conversion of **a** is reached within 10 and 5 min, respectively (Table 2, $\text{TOF} = 100,000\text{ h}^{-1}$ for both entries 1 and 2). However, with 10 equiv. ampy, the conversion decreases if the base NaO^iPr is added to

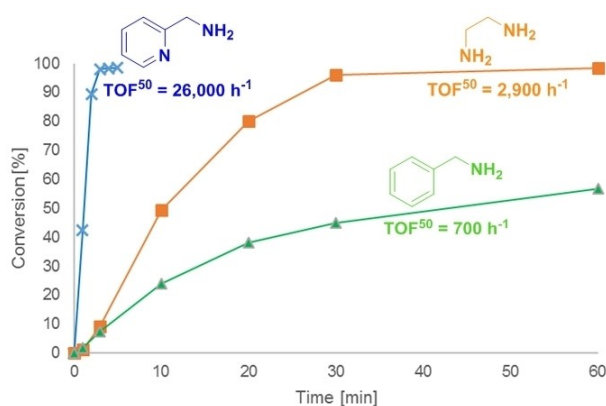


Figure 6. Transfer hydrogenation of acetophenone with complex **4** and 10 equiv. additives, ampy, en, bza. Conditions: $i\text{PrOH}$, 1 mmol **a**, 2 mol% NaO^iPr , 0.1 mol% **4**, 1.0 mol% additives, $S/C/B = 100/0.1/2$. x ampy, \blacksquare en, \blacktriangle bza.

| Entry | Catalyst | Catalyst loading [mol%] | ampy [equiv.] ^[b] | Conversion ^[c] [%] | Time [min] | $\text{TOF}^{[d]}$ [h^{-1}] |
|-------|----------|-------------------------|------------------------------|-------------------------------|------------|--|
| 1 | 4 | 0.03 | 2 | 96 | 10 | 100,000 |
| 2 | 4 | 0.03 | 10 | 96 | 5 | 100,000 |
| 3 | 6 | 0.03 | – | 99 | 5 | 125,000 |
| 4 | 6 | 0.02 | – | 98 | 5 | 103,000 |
| 5 | 6 | 0.01 | – | 87 | 10 | 105,300 |
| 6 | 7 | 0.03 | – | 4 | 240 | n.d. |

[a] Conditions: $i\text{PrOH}$, 1 mmol **a**, 2 mol% NaO^iPr , $S/B = 100/2$, [b] Maximum conversion, determined by GC; conversion corresponds to yield of 1-phenylethanol, [c] Calculated at 50% conversion.

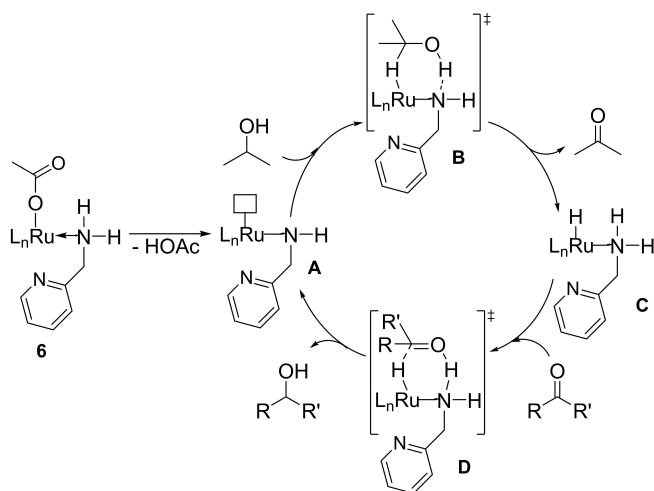
the refluxing mixture after 2 min, while consecutive addition of 10 equiv. ampy-catalyst-base produces the same high catalytic activities as observed with 2 equiv. ampy.

On account of the accelerating effect of ampy on catalyst **4**, the isolated ampy derivative **6** was examined at 0.03 mol% catalyst loading. Similar to the *in situ* system, **6** converts 98% **a** within 5 min with TOFs of $125,000\text{ h}^{-1}$ (Table 2, entry 3). At 0.02 mol% loading of **6**, full conversion is achieved after 5 min, with slightly lower rate ($\text{TOF} = 103,000\text{ h}^{-1}$, Table 2, entry 4), whereas at 0.01 mol% of **6**, 87% conversion of **a** is achieved in 10 min, reaching a TOF of $105,300\text{ h}^{-1}$ (Table 2, entry 5). By contrast to the high activity observed with the monodentate ampy complex **6**, the related bidentate ampy derivative **7** is practically inactive in the TH of **a**, converting only 4% of the substrate in 4 h (Table 2, entry 6). The low activity is likely due to the lack of a labile ligand in **7**, hindering the formation of the catalytically active hydride species via ruthenium isopropoxides.

To evaluate the substrate scope of the best-performing catalyst **6**, a variety of ketones was examined in the TH with 0.03 mol% **6** (Scheme 3, Table 3). In addition to **a** (Table 3, entry 1), the para-substituted acetophenone derivatives **b**, **c** and **d** with $R = \text{Me}$, MeO and Cl are fully converted in 10 min with TOFs between 55,000 and $75,300\text{ h}^{-1}$ (Table 3, entries 2–4). Derivatives **c** and **d** with electron-withdrawing groups (Table 3, entries 3 and 4) exhibit slightly higher TOFs than the electron-donating **b** (Table 3, entry 2). Ortho-substitution of acetophenone with a chloride moiety (substrate **e**) leads to comparable performance as with the unsubstituted derivative **a** (Table 3, entry 5). The order of activity of **6** in TH of acetophenone derivatives is thus $\text{a} > \text{e} > \text{b} > \text{c} > \text{d}$ ($R = \text{Me} > \text{MeO} > \text{Cl}$). The diaryl substrate benzophenone **f** is converted in 94% within 20 min as well ($\text{TOF} = 55,600\text{ h}^{-1}$, Table 3, entry 6). The slower rate is attributed to the steric hindrance of the substrate. Cyclic aliphatic ketones **g** and **h** are fully converted within 10 min, affording TOFs of 105,800 and $52,800\text{ h}^{-1}$, respectively (Table 3, entries 7 and 8). The linear ketone **i** is hydrogenated in 99% within 10 min ($\text{TOF} = 43,800\text{ h}^{-1}$, Table 3, entry 9), whereas the unsaturated ketone **j** is selectively reduced at the carbonyl functionality without formation of the saturated alcohol (Table 3, entry 10).

| Entry | Substrate | Conversion ^[b] [%] | Time [min] | $\text{TOF}^{[c]}$ [h^{-1}] |
|-------|-----------|-------------------------------|------------|--|
| 1 | a | 99 | 5 | 125,000 |
| 2 | b | 96 | 10 | 75,300 |
| 3 | c | 90 | 10 | 62,300 |
| 4 | d | 99 | 5 | 55,000 |
| 5 | e | 98 | 10 | 116,300 |
| 6 | f | 94 | 20 | 55,600 |
| 7 | g | 98 | 10 | 105,800 |
| 8 | h | 97 | 10 | 52,800 |
| 9 | i | 99 | 10 | 43,800 |
| 10 | j | 80 | 10 | 57,100 |

[a] Conditions: $i\text{PrOH}$, 1 mmol ketone substrate, 2 mol% NaO^iPr , 0.03 mol% **6**, $S/C/B = 100/0.03/2$, [b] Maximum conversion, determined by GC; conversion corresponds to yield of 1-phenylethanol, [c] Calculated at 50% conversion.



Scheme 4. Proposed catalytic cycle for ketone TH with **6**. $L_n = \text{dppb, acac}$.

In analogy to results obtained by *Noyori et al.* for ruthenium (II) primary amine complexes^[12] a bifunctional outer sphere mechanism is proposed for the catalytic TH of ketone derivatives with complex **6** (Scheme 4).

Accordingly, dissociation of acetate from **6** and deprotonation of ampy leads to the five-coordinated species **A** with a free coordination site that can be occupied by isopropanol through a six-membered transition state **B**. Oxidation of isopropanol and release of acetone results in the ruthenium hydride species **C**, which with the ketone substrate forms transition state **D**. Reduction of the substrate then regenerates species **A**. This proposed mechanism is in accordance with the high catalytic activity of ampy complex **6**, observed also for other ruthenium amine complexes that operate through bifunctional catalysis.^[17] The inactivity of catalyst precursors **5** and **7** is attributed to strong coordination of the bidentate ligands that inhibits the formation of a free coordination site as in **A**. *Baratta et al.* confirmed that an excess of isopropanol plays a crucial role for the formation of **B** and that the alcohol decreases the energy of the transition state, thus facilitating hydrogen transfer to the substrate.^[11a] Current studies are directed to the isolation of catalytic intermediate species from **6** in isopropanol.

Conclusion

The mixed ruthenium(II) acetate/acetylacetonate phosphine complexes $\text{Ru}(\text{OAc})(\text{acac})\text{P}_2$ ($\text{P}_2 = (\text{PPh}_3)_2, \text{dppb}$) can be easily synthesized and are examined in catalytic ketone transfer hydrogenation reactions with isopropanol. In comparison to the corresponding diacetate complexes, the performance of the mixed catalysts is superior in terms of stability and activity, while the diacetylacetonate $\text{Ru}(\text{acac})_2(\text{dppb})$ appears not active. Higher activity is found for the ampy derivative $\text{Ru}(\text{OAc})(\text{acac})(\text{ampy})(\text{dppb})$ (**6**), reaching TOFs of $125,000 \text{ h}^{-1}$ for the reduction of a number of aliphatic and aromatic ketones at loadings as low as 0.01 mol%. Ongoing studies focus on the develop-

ment of easily accessible carboxylate ruthenium complexes in combination with 2-(aminomethyl)pyridine for catalytic organic transformations.

Experimental Section

All reactions were carried out under argon atmosphere using standard Schlenk techniques. Solvents were used after distillation or taken from a solvent purification system (SPS) from *MBraun*, degassed and stored over mole sieves (3 and 4 Å). Ketone substrates for catalytic reactions were degassed prior to use. Ruthenium precursors were obtained from *Johnson Matthey Ltd.* and all other chemicals were purchased from *Sigma Aldrich*, *Merck* and *abcr*. $\text{Ru}(\text{OAc})_2(\text{PPh}_3)_2$ (**1**) and $\text{Ru}(\text{OAc})_2(\text{dppb})$ (**2**) were synthesized following adapted literature procedures.^[1d,15] NMR measurements were recorded on *Bruker AV-400* and *AC-200* instruments. Chemical shifts in ppm are reported relative to the stated solvent for ^1H and ^{13}C spectra and relative to H_3PO_4 for ^{31}P spectra. Elemental analyses (C, H, N) were carried out on a *Varian SpectraAA-400* instrument and on a *Flash EA1112* elemental analyzer from *Carlo Erba*. GC analyses were performed on an *Agilent 7890B* gas chromatograph equipped with an *HP-5* column with 30 m length, column pressure 5 psi, Ar as carrier gas, and a flame ionization detector (FID). The injector and detector temperatures were 300°C , with initial $T = 80^\circ\text{C}$ ramped to 138°C at $8^\circ\text{C}/\text{min}$ and then to 300°C at $30^\circ\text{C}/\text{min}$.

Syntheses of ruthenium(II) diphosphine complexes

Synthesis of $\text{Ru}(\text{OAc})(\text{acac})(\text{PPh}_3)_2$ (3**).** To a solution of 100 mg of $\text{Ru}(\text{OAc})_2(\text{PPh}_3)_2$ (**1**) (1.0 equiv., 0.134 mmol) in 3 mL dichloromethane, 21 μL of pentane-2,4-dione (20.0 mg, 1.5 equiv., 0.202 mmol) are added. The mixture is stirred at 30°C for 3 h and then concentrated to ca. 0.5 mL and the product precipitated in 3 mL pentane. Filtration and washing with pentane ($3 \times 0.5 \text{ mL}$) affords 68% of complex **3** (71.3 mg, 0.091 mmol) as an orange solid. El. Anal. Calcd. for $\text{C}_{43}\text{H}_{40}\text{O}_4\text{P}_2\text{Ru}$: C, 65.89; H, 5.14. Found: C, 65.90; H, 5.15. $^1\text{H-NMR}$ (200 MHz, CDCl_3 , 293 K): δ (ppm) = 6.39–7.68 (m, 30H, aromatic protons), 5.10 (s, 1H, CH), 1.69 (s, 3H, CH_3), 1.59 (s, 3H, CH_3), 1.47 (s, 3H, CH_3). $^{13}\text{C}\{^1\text{H}\}\text{-NMR}$ (50 MHz, CDCl_3 , 293 K): δ (ppm) = 187.6 (s, COCH_3), 187.0 (s, COCH_3), 185.8 (s, O_2C), 133.74–135.23 (m, aromatic carbon atoms), 128.7 (d, $^3J(\text{CP}) = 2.3 \text{ Hz}$, aromatic carbon atoms), 127.3 (d, $^3J(\text{CP}) = 9.2 \text{ Hz}$, aromatic carbon atoms), 100.0 (s, CH), 27.6 (s, CH_3), 23.9 (s, CH_3). $^{31}\text{P}\{^1\text{H}\}\text{-NMR}$ (81 MHz, CDCl_3 , 293 K): δ (ppm) = 64.9 (d, $^2J(\text{PP}) = 36.4 \text{ Hz}$), 53.5 (d, $^2J(\text{PP}) = 36.4 \text{ Hz}$).

Synthesis of $\text{Ru}(\text{OAc})(\text{acac})(\text{dppb})$ (4**).** To a solution of 300 mg of $\text{Ru}(\text{OAc})_2(\text{dppb})$ (**2**) (1.0 equiv., 0.465 mmol) in 9 mL dichloromethane, 286 μL of pentane-2,4-dione (279 mg, 6.0 equiv., 2.79 mmol) are added. The mixture is stirred at 30°C for 3 h and then concentrated to ca. 0.5 mL and precipitated in 8 mL pentane. Decantation and washing with pentane ($5 \times 3 \text{ mL}$) affords 63% of complex **4** (199 mg, 0.290 mmol) as a yellow solid. Crystals are obtained by dilution of the solid in dichloromethane and storing under *n*-heptane atmosphere. El. Anal. Calcd. for $\text{C}_{35}\text{H}_{38}\text{O}_4\text{P}_2\text{Ru}$: C, 61.31; H, 5.59. Found: C, 61.68; H, 5.67. $^1\text{H-NMR}$ (200 MHz, CDCl_3 , 293 K): δ (ppm) = 6.43–8.12 (m, 20H, aromatic protons), 5.05 (s, 1H, CH), 1.83–3.03 (m, 8H, CH_2), 1.68 (s, 3H, CH_3), 1.52 (s, 3H, CH_3), 1.45 (s, 3H, CH_3). $^{13}\text{C}\{^1\text{H}\}\text{-NMR}$ (50 MHz, CDCl_3 , 293 K): δ (ppm) = 187.0 (s, O_2C), 186.2 (s, COCH_3), 185.6 (s, COCH_3), 124.4–135.20 (m, aromatic carbon atoms), 99.8 (s, CH), 27.7–28.9 (m, CH_2), 27.5 (s, CH_3), 24.0 (s, CH_3), 23.3 (d, $^2J(\text{CP}) = 41.8 \text{ Hz}$, CH_2). $^{31}\text{P}\{^1\text{H}\}\text{-NMR}$ (81 MHz, CDCl_3 , 293 K): δ (ppm) = 66.8 (d, $^2J(\text{PP}) = 43.2 \text{ Hz}$), 52.6 (d, $^2J(\text{PP}) = 43.2 \text{ Hz}$).

Synthesis of Ru(acac)₂(dppb) (5). A solution of 75 mg of Ru(OAc)₂(dppb) (2) (1.0 equiv., 0.116 mmol) and 72 μL of pentane-2,4-dione (6.0 equiv., 70 mg, 0.697 mmol) is stirred in 3 mL dichloromethane at 30 °C for 3 d. The solution is concentrated to ca. 0.5 mL and the product precipitated in 2 mL pentane. Decantation with pentane (5 × 0.5 mL) and drying *in vacuo* affords 58% of complex 5 (49 mg, 0.067 mmol) as an orange solid. El. Anal. Calcd. for C₃₈H₄₂O₄P₂Ru: C, 62.89; H, 5.83. Found: C, 62.65; H, 5.84. ¹H-NMR (200 MHz, CD₂Cl₂, 293 K): δ (ppm) = 7.51–8.11 (m, 4H, aromatic protons), 7.24–7.48 (m, 6H, aromatic protons), 7.04–7.22 (m, 10H, aromatic protons), 4.92 (s, 2H, CH), 2.00–2.48 (m, 8H, CH₂), 1.65 (s, 6H, CH₃), 1.46 (s, 6H, CH₃). ¹³C{¹H}-NMR (50 MHz, CDCl₃, 293 K): δ (ppm) = 185.5 (s, COCH₃), 184.3 (s, COCH₃), 139.0–141.2 (m, aromatic carbon atoms), 136.6–138.7 (m, aromatic carbon atoms), 134.3 (t, ¹J(CP) = 4.4 Hz, aromatic carbon atoms), 132.4 (t, ¹J(CP) = 4.4 Hz, aromatic carbon atoms), 128.9 (s, aromatic carbon atoms), 127.9 (s, aromatic carbon atoms), 127.2 (dt, ¹J(CC) = 8.8 Hz, 4.4 Hz, aromatic carbon atoms), 98.8 (s, CH), 28.1–29.6 (m, CH₂), 27.9 (s, CH₃), 26.6–27.8 (m, CH₂), 23.5 (s, CH₃). ³¹P{¹H}-NMR (81 MHz, CDCl₃, 293 K): δ (ppm) = 52.9 (s).

Synthesis of Ru(OAc)(acac)(ampy)(dppb) (6). A solution of 50 mg Ru(OAc)(acac)(dppb) (4) (1.0 equiv., 0.073 mmol) and 45 μL 2-(aminomethyl)pyridine (6.0 equiv., 47 mg, 0.438 mmol) in 2 mL dichloromethane is stirred at room temperature for 6 h. The solution is then concentrated to ca. 0.5 mL and orange crystals of 6 * CH₂Cl₂ are obtained in 77% yield (49 mg, 0.056 mmol) by slow diffusion of 3 mL pentane to the solution at 4 °C. El. Anal. Calcd. for C₄₂H₄₈Cl₂N₂O₄P₂Ru: C, 57.41; H, 5.51; N, 3.19. Found: C, 57.54; H, 5.69; N, 3.46. ¹H-NMR (400 MHz, tol-d₈, 293 K): δ (ppm) = 8.19 (dt, ³J = 4.80 Hz, ⁴J = 1.46 Hz, 1H, py-H₆), 8.03 (td, ³J = 8.52 Hz, ⁴J = 1.42 Hz, 2H, H_{ph}), 7.83–7.69 (m, 2H, H_{ph}), 7.69–7.49 (m, 2H, H_{ph}), 7.34–6.87 (m, 15H, py-H₄, H_{ph}), 6.92–6.97 (m, 1H, NH₂), 6.80 (d, ³J = 7.83 Hz, 1H, py-H₃), 6.50 (ddd, ³J = 7.62 Hz, ³J = 4.80 Hz, ⁴J = 1.19 Hz, 1H, py-H₅), 4.92 (s, 1H, CH), 4.30 (s, 2H, CH₂Cl₂), 3.98 (t, ³J = 11.72 Hz, 1H, NH₂), 3.77 (ddd, ²J = 15.23 Hz, ³J = 11.72 Hz, ⁴J = 3.76 Hz, 1H, CH₂NH₂), 3.37 (ddd, ²J = 15.23 Hz, ³J = 11.72 Hz, ⁴J = 3.12 Hz, 1H, CH₂NH₂), 2.85–2.36 (m, 3H, CH₂^{dppb}), 2.16 (s, 3H, O₂CCH₃), 1.90–1.70 (m, 2H, CH₂^{dppb}), 1.64 (s, 3H, COCH₃), 1.61–1.34 (m, 3H, CH₂^{dppb}), 1.33 (s, 3H, COCH₃). ¹³C{¹H}-NMR (101 MHz, tol-d₈, 293 K): δ (ppm) = 185.8 (s, COCH₃), 185.5 (s, COCH₃), 181.2 (s, O₂C), 161.4 (s, py-C₂), 149.0 (s, py-C₆), 135.8 (s, py-C₄), 135.2 (d, ³J(CP) = 8.9 Hz, C_{ph}), 134.4 (d, ³J(CP) = 8.9 Hz, C_{ph}), 133.6 (d, ³J(CP) = 8.9 Hz, C_{ph}), 133.0 (d, ³J(CP) = 8.9 Hz, C_{ph}), 127.3 (t, ⁴J(CP) = 7.7 Hz, C_{ph}), 121.3 (s, py-C₃, py-C₅), 100.3 (s, CH), 53.3 (s, CH₂Cl₂), 47.4 (s, CH₂NH₂), 27.7–27.8 (m, COCH₃), 27.3 (s, COCH₃), 26.1 (s, O₂CCH₃), 24.6 (s, CH₂^{dppb}), 22.3 (s, CH₂^{dppb}). ³¹P{¹H}-NMR (162 MHz, tol-d₈, 263 K): δ (ppm) = 53.2 (d, ²J(PP) = 38.2 Hz), 45.9 (d, ²J(PP) = 38.2 Hz).

Synthesis of [Ru(acac)(ampy)(dppb)](OAc) (7). A solution of 100 mg Ru(OAc)(acac)(ampy)(dppb)*CH₂Cl₂ (6) (1.0 equiv., 0.114 mmol) in 4 mL toluene is heated to 90 °C for 1 h. After cooling to room temperature, the solution is concentrated to ca. 0.5 mL and coated with 4 mL pentane. Cooling to 2 °C for 2 d affords 7 as an orange-brown precipitate in 85% yield (77 mg, 0.097 mmol). El. Anal. Calcd. for C₄₁H₄₆N₂O₄P₂Ru: C, 62.03; H, 5.84; N, 3.53. Found: C, 61.91; H, 6.23; N, 3.54. ¹H-NMR (400 MHz, tol-d₈, 293 K): δ (ppm) = 8.63–8.46 (m, 1H, NH), 8.12 (t, ³J = 8.48 Hz, 2H, H_{ph}), 8.08–8.01 (m, 1H, py-H₆), 7.74 (t, ³J = 8.27 Hz, 2H, H_{ph}), 7.56 (ddd, ³J = 9.70 Hz, ³J = 8.19 Hz, ⁴J = 1.64 Hz, 2H, H_{ph}), 7.40 (t, ³J = 8.27 Hz, 2H, H_{ph}), 7.30–7.13 (m, 5H, H_{ph}), 6.94 (ddd, ³J = 8.48 Hz, ³J = 6.25 Hz, ⁴J = 1.64 Hz, 4H, H_{ph}), 6.83–6.65 (m, 3H, H_{ph}), 6.46 (td, ³J = 7.77 Hz, ⁴J = 1.60 Hz, 1H, py-H₄), 6.21 (t, ³J = 6.59 Hz, 1H, py-H₅), 5.91 (d, ³J = 7.77 Hz, 1H, py-H₃), 4.96 (s, 1H, CH), 4.15 (tt, ²J = 12.05 Hz, ³J = 5.76 Hz, 1H, CH₂^{dppb}), 3.99–3.84 (m, 1H, CH₂^{dppb}), 3.84–3.66 (m, 1H, CH₂NH₂), 3.53 (dd, ²J = 18.18 Hz, ³J = 8.34 Hz, 1H, CH₂NH₂), 3.41–3.26 (m, 1H, NH), 2.82–2.53 (m, 2H, CH₂^{dppb}), 2.53 (s, 3H, O₂CCH₃), 1.94 (s, 3H, COCH₃), 1.60–1.09 (m, 4H, CH₂^{dppb}), 1.02 (s, 3H, COCH₃). ¹³C{¹H}-NMR (101 MHz, tol-d₈, 293 K): δ

(ppm) = 185.8 (s, COCH₃), 185.4 (s, COCH₃), 176.9 (s, O₂C), 165.0 (s, py-C₂), 146.9 (s, py-C₆), 135.2 (s, py-C₄), 135.2 (t, ²J(CP) = 10.7 Hz), 134.8 (d, ³J(CP) = 9.4 Hz, C_{ph}), 132.2 (d, ³J(CP) = 8.3 Hz, C_{ph}), 131.6 (d, ³J(CP) = 8.3 Hz, C_{ph}), 129.5 (m, C_{ph}), 121.3 (s, py-C₅), 120.6 (s, py-C₃), 100.1 (s, CH), 52.0 (s, CH₂NH₂), 28.7 (s, CH₂^{dppb}), 28.4 (s, COCH₃), 27.4 (s, COCH₃), 25.7 (s, O₂CCH₃), 25.5 (s, CH₂^{dppb}). ³¹P{¹H}-NMR (162 MHz, tol-d₈, 293 K): δ (ppm) = 51.0 (d, ²J(PP) = 36.8 Hz), 45.6 (d, ²J(PP) = 36.8 Hz).

Procedure for the catalytic transfer hydrogenation of acetophenone

Ruthenium complexes (1.0–0.1 μmol) were dissolved in 10 mL ⁱPrOH under argon. 2-(Aminomethyl)pyridine (15.4 μL) was stirred in 15 mL ⁱPrOH. The ketone substrate (1 mmol) was placed in a Schlenk flask closed by a rubber septum under argon and dissolved in ⁱPrOH (final volume of the solution 10 mL). The solution was then heated to 90 °C oil bath temperature under argon. After consecutive addition of the respective amount of ampy solution (where applicable), catalyst solution and 200 μL NaOⁱPr in ⁱPrOH (0.1 M; 0.02 mmol), the reduction of the ketone started immediately. The reaction was sampled by removing an aliquot of the reaction mixture under constant argon flow, and diethyl ether was added to the sample (1/1, v/v). The solution was filtered over a short silica pad and the conversion determined by GC analysis (Ru 0.1–0.01 mol%, ampy 1–0.02 mol%, NaOⁱPr 2 mol%, acetophenone 0.1 M).

Acknowledgements

The authors thank Marike Drexler, Wenyi Zeng and Alexandra Walter for help with catalytic experiments. The TUM Graduate Schools of Chemistry and MSE are gratefully acknowledged for financial support for D.A.H., E.-M.H.J.E. and P.J.F.

Conflict of Interest

The authors declare no conflict of interest.

Keywords: acetylacetonate · 2-(aminomethyl)pyridine · hydrogenation · ruthenium complexes · transfer hydrogenation

- [1] a) M. Bianchi, P. Frediani, U. Matteoli, G. Menchi, F. Piacenti, G. Petrucci, *J. Organomet. Chem.* **1983**, *259*, 207–214; b) D. A. Hey, P. J. Fischer, W. Baratta, F. E. Kühn, *Dalton Trans.* **2019**, *48*, 4625–4635; c) M. Kitamura, T. Ohkuma, S. Inoue, N. Sayo, H. Kumobayashi, S. Akutagawa, T. Ohta, H. Takaya, R. Noyori, *J. Am. Chem. Soc.* **1988**, *110*, 629–631; d) R. W. Mitchell, A. Spencer, G. Wilkinson, *Dalton Trans.* **1973**, 846–854; e) M. Naruto, S. Saito, *Nat. Commun.* **2015**, *6*, 8140.
- [2] a) M. Kitamura, M. Tsukamoto, Y. Bessho, M. Yoshimura, U. Kobs, M. Widhalm, R. Noyori, *J. Am. Chem. Soc.* **2002**, *124*, 6649–6667; b) L. Pardatscher, M. J. Bitzer, C. Jandl, J. W. Kück, R. M. Reich, F. E. Kühn, W. Baratta, *Dalton Trans.* **2019**, *48*, 79–89; c) J. Witt, A. Pöthig, F. E. Kühn, W. Baratta, *Organometallics* **2013**, *32*, 4042–4045.
- [3] T. Ohta, H. Takaya, R. Noyori, *Inorg. Chem.* **1988**, *27*, 566–569.
- [4] a) S. Giboulot, S. Baldino, M. Ballico, R. Figliolia, A. Pöthig, S. Zhang, D. Zuccaccia, W. Baratta, *Organometallics* **2019**, *38*, 1127–1142; b) D. A. Hey, R. M. Reich, W. Baratta, F. E. Kühn, *Coord. Chem. Rev.* **2018**, *374*, 114–132; c) L. Pardatscher, B. J. Hofmann, P. J. Fischer, S. M. Hölzl, R. M. Reich, F. E. Kühn, W. Baratta, *ACS Catal.* **2019**, *9*, 11302–11306.

- [5] a) A. K. Gupta, R. K. Poddar, *Indian J. Chem. Sect. A* **2000**, *39*, 457–460; b) M. A. Bennett, M. J. Byrnes, G. Chung, A. J. Edwards, A. C. Willis, *Inorg. Chim. Acta* **2005**, *358*, 1692–1708.
- [6] a) M. A. Bennett, G. Chung, D. C. R. Hockless, H. Neumann, A. C. Willis, *Dalton Trans.* **1999**, 3451–3462; b) R. D. Ernst, E. Melendez, L. Stahl, M. L. Ziegler, *Organometallics* **1991**, *10*, 3635–3642; c) C. Grunwald, M. Laubender, J. Wolf, H. Werner, *Dalton Trans.* **1998**, *5*, 833–839.
- [7] T. Manimaran, T. C. Wu, W. D. Klobucar, C. H. Kolich, G. P. Stahly, F. R. Fronczek, S. E. Watkins, *Organometallics* **1993**, *12*, 1467–1470.
- [8] a) J. R. Cabrero-Antonino, E. Alberico, K. Junge, H. Junge, M. Beller, *Chem. Sci.* **2016**, *7*, 3432–3442; b) C.-C. Chen, T.-T. Huang, C.-W. Lin, R. Cao, A. S. C. Chan, W. T. Wong, *Inorg. Chim. Acta* **1998**, *270*, 247–251.
- [9] T. Ohta, H. Takaya, M. Kitamura, K. Nagai, R. Noyori, *J. Org. Chem.* **1987**, *52*, 3174–3176.
- [10] a) E. Peris, *Chem. Rev.* **2018**, *118*, 9988–10031; b) B. Zhao, Z. Han, K. Ding, *Angew. Chem. Int. Ed.* **2013**, *52*, 4744–4788; *Angew. Chem.* **2013**, *125*, 4844–4889.
- [11] a) W. Baratta, S. Baldino, M. J. Calhorda, P. J. Costa, G. Esposito, E. Herdtweck, S. Magnolia, C. Mealli, A. Messaoudi, S. A. Mason, L. F. Veiros, *Chem. Eur. J.* **2014**, *20*, 13603–13617; b) W. Baratta, E. Herdtweck, K. Siega, M. Toniutti, P. Rigo, *Organometallics* **2005**, *24*, 1660–1669; c) W. Baratta, P. Rigo, *Eur. J. Inorg. Chem.* **2008**, *2008*, 4041–4053.
- [12] R. Noyori, M. Yamakawa, S. Hashiguchi, *J. Org. Chem.* **2001**, *66*, 7931–7944.
- [13] a) S. Baldino, S. Facchetti, A. Zanotti-Gerosa, H. G. Nedden, W. Baratta, *ChemCatChem* **2016**, *8*, 2279–2288; b) G. Chelucci, S. Baldino, W. Baratta, *Coord. Chem. Rev.* **2015**, *300*, 29–85; c) S. Giboulot, S. Baldino, M. Ballico, H. G. Nedden, D. Zuccaccia, W. Baratta, *Organometallics* **2018**, *37*, 2136–2146.
- [14] a) Á. Vivancos, C. Segarra, M. Albrecht, *Chem. Rev.* **2018**, *118*, 9493–9586; b) Z. Wei, H. Jiao, *Advances in Inorganic Chemistry, Vol. 73* (Eds.: R. van Eldik, R. Puchta), Academic Press **2019**, pp. 323–384; c) R. Figliolia, P. Cavigli, C. Comuzzi, A. Del Zotto, D. Lovison, P. Strazzolini, S. Susmel, D. Zuccaccia, M. Ballico, W. Baratta, *Dalton Trans.* **2020**, *49*, 453–465.
- [15] R. Figliolia, S. Baldino, H. G. Nedden, A. Zanotti-Gerosa, W. Baratta, *Chem. Eur. J.* **2017**, *23*, 14416–14419.
- [16] W. Baratta, M. Ballico, A. Del Zotto, E. Herdtweck, S. Magnolia, R. Peloso, K. Siega, M. Toniutti, E. Zangrando, P. Rigo, *Organometallics* **2009**, *28*, 4421–4430.
- [17] B. Zhao, Z. Han, K. Ding, *Angew. Chem. Int. Ed.* **2013**, *52*, 4744–4788; *Angew. Chem.* **2013**, *125*, 4844–4889.

Manuscript received: March 29, 2020

Revised manuscript received: April 17, 2020

Accepted manuscript online: April 18, 2020

Version of record online: May 19, 2020